

Note: This copy is for your personal non-commercial use only. To order presentation-ready copies for distribution to your colleagues or clients, contact us at [www.rsna.org/lrsnarights](http://www.rsna.org/lrsnarights).

# Intraprocedural C-Arm Dual-Phase Cone-Beam CT: Can It Be Used to Predict Short-term Response to TACE with Drug-eluting Beads in Patients with Hepatocellular Carcinoma?<sup>1</sup>

Romaric Loffroy, MD, PhD  
MingDe Lin, PhD  
Gayane Yenokyan, PhD  
Pramod P. Rao, MD  
Nikhil Bhagat, MD  
Niels Noordhoek, PhD  
Alessandro Radaelli, PhD  
Järl Blijd, MSc  
Eleni Liapi, MD  
Jean-François Geschwind, MD

<sup>1</sup>From the Russell H. Morgan Department of Radiology and Radiological Science, Division of Vascular and Interventional Radiology, Johns Hopkins Hospital, Sheikh Zayed Tower, Ste 7203, 1800 Orleans St, Baltimore, MD 21287 (R.L., P.P.R., N.B., E.L., J.F.G.); Clinical Informatics, Interventional, and Translational Solutions (CIITS), Philips Research North America, Briarcliff Manor, NY (M.L.); Johns Hopkins Biostatistics Center, Johns Hopkins Bloomberg School of Public Health, Baltimore, MD (G.Y.); and Philips Healthcare, Best, the Netherlands (N.N., A.R., J.B.). Received October 31, 2011; revision requested January 10, 2012; revision received March 23; accepted June 5; final version accepted July 11. Supported by the French Society of Radiology and by a grant from Philips Research North America, Briarcliff Manor, NY. **Address correspondence to J.F.G.** (e-mail: [jfg@jhmi.edu](mailto:jfg@jhmi.edu)).

This publication was made possible by a grant from the National Center for Research Resources (NCR), a component of the National Institutes of Health (NIH), and the NIH Roadmap for Medical Research. Its contents are solely the responsibility of the authors and do not necessarily represent the official view of NCR or NIH.

© RSNA, 2012

## Purpose:

To investigate whether C-arm dual-phase cone-beam computed tomography (CT) performed during transcatheter arterial chemoembolization (TACE) with doxorubicin-eluting beads can help predict tumor response at 1-month follow-up in patients with hepatocellular carcinoma (HCC).

## Materials and Methods:

This prospective study was compliant with HIPAA and approved by the institutional review board and animal care and use committee. Analysis was performed retrospectively on 50 targeted HCC lesions in 29 patients (16 men, 13 women; mean age, 61.9 years  $\pm$  10.7) treated with TACE with drug-eluting beads. Magnetic resonance (MR) imaging was performed at baseline and 1 month after TACE. Dual-phase cone-beam CT was performed before and after TACE. Tumor enhancement at dual-phase cone-beam CT in early arterial and delayed venous phases was assessed retrospectively with blinding to MR findings. Tumor response at MR imaging was assessed according to European Association for the Study of the Liver (EASL) guidelines. Two patients were excluded from analysis because dual-phase cone-beam CT scans were not interpretable. Logistic regression models for correlated data were used to compare changes in tumor enhancement between modalities. The radiation dose with dual-phase cone-beam CT was measured in one pig.

## Results:

At 1-month MR imaging follow-up, complete and/or partial tumor response was seen in 74% and 76% of lesions in the arterial and venous phases, respectively. Paired *t* tests used to compare images obtained before and after TACE showed a significant reduction in tumor enhancement with both modalities ( $P < .0001$ ). The decrease in tumor enhancement seen with dual-phase cone-beam CT after TACE showed a linear correlation with MR findings. Estimated correlation coefficients were excellent for first ( $R = 0.89$ ) and second ( $R = 0.82$ ) phases. A significant relationship between tumor enhancement at cone-beam CT after TACE and complete and/or partial tumor response at MR imaging was found for arterial (odds ratio, 0.95; 95% confidence interval [CI]: 0.91, 0.99;  $P = .023$ ) and venous (odds ratio, 0.96; 95% CI: 0.93, 0.99;  $P = .035$ ) phases with the multivariate logistic regression model. Radiation dose for two dual-phase cone-beam CT scans was 3.08 mSv.

## Conclusion:

Intraprocedural C-arm dual-phase cone-beam CT can be used immediately after TACE with doxorubicin-eluting beads to predict HCC tumor response at 1-month MR imaging follow-up.

©RSNA, 2012

**H**epatocellular carcinoma (HCC) is the third most common cause of cancer death worldwide (1). Most patients present with intermediate or advanced disease that is not amenable to curative treatment, and the median survival in this group is 6–8 months (2). Several studies and well-designed randomized trials have shown a positive effect of transcatheter arterial chemoembolization (TACE) on patient outcome and survival (3–11).

Early assessment of the effectiveness of TACE and monitoring of tumor response are paramount to the identification of treatment failure, guidance of future therapy, and determination of the interval for repeat treatment. Response is typically evaluated with computed tomography (CT) or magnetic resonance (MR) imaging 1–3 months after TACE by using Response Evaluation Criteria in Solid Tumors (RECIST) guidelines (12–14). However, assessment of anatomic response in the early posttreatment period can be misleading because the absence of a reduction in tumor size does not mean an absence of response and often does not correlate with the degree of tumor necrosis (15,16). Consequently, a reduction in tumor enhancement at imaging has been used more accurately as a biomarker of tumor response, as proposed

by the European Association for the Study of the Liver (EASL) (15,17). Because the response to TACE is typically evaluated with MR imaging 1 month after treatment at our institution (in rare cases in which MR imaging cannot be performed, CT is used instead), it is too late for intraoperative treatment modification. This is especially problematic if patients must undergo repeat treatment. Imaging control after TACE with doxorubicin-eluting beads can also be made soon after the procedure (eg, the next day) with CT or MR imaging. However, a real-time (ie, at the time of treatment) imaging modality that could serve as an early surrogate marker of tumor necrosis and that could be used to predict future tumor response would be immensely beneficial, especially because treatment response has been identified as an independent predictor of survival (3). Recently, C-arm CT has emerged as a new and widely used imaging technology in the angiography suite, enabling the acquisition of a three-dimensional data set generated from one rotational run with use of cone-beam CT principles (18–22). Early clinical experience has demonstrated C-arm CT to be a useful adjunct to digital subtraction angiography (DSA) for use in hepatic vascular intervention procedures (18,21). It can be used to visualize tumor-feeding vessels and parenchymal stain during TACE. All current commercially available cone-beam CT systems necessitate two separate contrast material-enhanced scans. A recent development, which is vendor specific, is the ability to capture images during these two phases by using only one contrast material injection with C-arm dual-phase cone-beam CT (23–25). The new aspect of this proprietary technology is the addition of software

that enables the acquisition of two sequential, back-to-back cone-beam CT scans so images in both arterial and venous phases are captured by using only one contrast material injection. To our knowledge, no study has demonstrated whether dual-phase cone-beam CT technology could be used during TACE to predict tumor response.

We tested the hypotheses that the percentage change in tumor enhancement can be assessed at TACE with doxorubicin-eluting beads by using intraoperative C-arm dual-phase cone-beam CT technology and that this percentage can be used to predict anatomic changes at conventional MR imaging 1 month after TACE. More specifically, our objective was to investigate whether intraoperative C-arm dual-phase cone-beam CT performed during TACE with doxorubicin-eluting beads can be used to predict tumor response at 1-month follow-up in patients with HCC.

### Advances in Knowledge

- Dual-phase cone-beam CT provides images in both the early arterial and delayed venous phases with only one contrast material injection during transcatheter arterial chemoembolization (TACE) with doxorubicin-eluting beads in patients with hepatocellular carcinoma (HCC).
- Our study demonstrated a significant relationship between tumor enhancement seen at dual-phase cone-beam CT after TACE and objective MR imaging response (complete and partial response) at 1-month follow-up, suggesting that dual-phase cone-beam CT can be used to predict tumor response after TACE.

### Implication for Patient Care

- The dual-phase cone-beam CT technique can be included in the treatment paradigm because it can be used to predict short-term tumor response in patients with HCC treated with TACE with doxorubicin-eluting beads.

### Materials and Methods

Our study was financially supported by Philips Research North America,

#### Published online before print

10.1148/radiol.12112316 Content code: VA

Radiology 2013; 266:636–648

#### Abbreviations:

AFP =  $\alpha$ -fetoprotein

CI = confidence interval

DSA = digital subtraction angiography

EASL = European Association for the Study of the Liver

HCC = hepatocellular carcinoma

RECIST = Response Evaluation Criteria in Solid Tumors

TACE = transcatheter arterial chemoembolization

#### Author contributions:

Guarantor of integrity of entire study, J.F.G.; study concepts/study design or data acquisition or data analysis/interpretation, all authors; manuscript drafting or manuscript revision for important intellectual content, all authors; manuscript final version approval, all authors; literature research, R.L., M.L., J.F.G.; clinical studies, R.L., M.L., A.R., J.B., J.F.G.; experimental studies, M.L., P.P.R., N.N., A.R., E.L., J.F.G.; statistical analysis, R.L., G.Y., N.N.; and manuscript editing, R.L., M.L., N.B., A.R., J.B., E.L., J.F.G.

#### Funding:

This research was supported by the National Institutes of Health (grants NCI R01 CA160771 and UL1 RR 025005).

Conflicts of interest are listed at the end of this article.

Briarcliff Manor, NY. The authors who are not employees of Philips (R.L., G.Y., P.P.R., N.B., E.L., J.F.G.) had control of inclusion of any data and information submitted for publication that might present a conflict of interest for authors who are employees of Philips (M.L., N.N., A.R., J.B.).

### Study Cohort

This was a single-institution prospective study in which the data analysis was performed retrospectively. The study was compliant with the Health Insurance Portability and Accountability Act and was approved by the institutional review board. All patients provided written informed consent before inclusion in the study. The study group included all patients with HCC who qualified to undergo their first TACE procedure, who had not previously undergone systemic therapy, and who had undergone dynamic contrast-enhanced MR imaging before and approximately 1 month after TACE and intraoperative dual-phase cone-beam CT before and after TACE from March 2, 2009, to April 5, 2010. Patients were considered eligible for TACE if the diagnosis of HCC was confirmed by means of biopsy or typical radiologic findings. Additional eligibility criteria included an elevated serum  $\alpha$ -fetoprotein (AFP) level ( $>400$  ng/mL); Eastern Cooperative Oncology Group performance status of up to 2; Child-Pugh class A, B, or C disease; focal or multifocal hepatic malignancy; absent or trace ascites; albumin level of more than 2.5 g/dL; alanine aminotransferase and aspartate aminotransferase levels of less than five times the upper normal limit; total serum bilirubin level of less than 3.0 mg/dL; serum creatinine level of less than 2.0 mg/dL; platelet count of at least 50,000/mm<sup>3</sup>; international normalized ratio of up to 1.5; left ventricle ejection fraction of at least 50% (all patients underwent echocardiography); at least partial patency of the portal venous system; and no contraindications to MR imaging. Only patients with well-defined tumors were included in the study. Patients with small tumors ( $<1$  cm in diameter) ( $n = 2$ ) were excluded from our study

because enhancement of these tumors was difficult to assess. Patients who had previously undergone TACE ( $n = 16$ ) were also excluded because of a partial response to previous therapy. Lastly, patients with poor dual-phase cone-beam CT image quality ( $n = 2$ ) because of severe image artifacts were also excluded. In total, 27 patients were included in our study.

### TACE Protocol

All TACE procedures were performed by two experienced interventional radiologists (J.F.G. and N.B., with 13 and 5 years of experience, respectively) by using a consistent approach. LC Beads (2 mL; BioCompatibles, Surrey, United Kingdom) with a diameter of 100–300  $\mu$ m were loaded with 100 mg of doxorubicin hydrochloride (25 mg/mL) and mixed with an equal volume of nonionic contrast material (Oxilan, 300 mg of iodine per milliliter; Guerbet, Bloomington, Ind), as reported previously (10). Access to the common femoral artery was obtained with the Seldinger technique, and a catheter was positioned as close to the tumor bed as possible before infusion of the doxorubicin-eluting beads. This means that every injection was performed in a superselective (20 patients) or selective (seven patients, four in the right hepatic artery and three in the left hepatic artery) manner in the case of unifocal lesions or those with multiple feeding vessels, respectively, by using a microcatheter. In patients with larger tumors, the position of the microcatheter was changed within one session if necessary, and both segmental TACE and subsegmental TACE were performed. Doxorubicin-eluting beads (up to 100 mg) were administered by alternating aliquot injections of the beads and contrast material until complete delivery was achieved or the blood flow of the feeding artery slowed down substantially as an end point of the treatment. Complete occlusion of the main feeding artery was avoided to allow for repeat treatment if necessary, as has been reported before with a conventional TACE technique (26). This end point was altered on the basis of the dual-phase cone-beam CT findings

only if tumor enhancement was not decreased after treatment. On the other hand, we did not recommend further embolization in patients who showed substantial postprocedural enhancement at dual-phase cone-beam CT in the same setting.

### C-Arm Dual-Phase Cone-Beam CT Technique

All patients underwent C-arm dual-phase cone-beam CT before and immediately after TACE. Imaging was performed by using a commercially available angiographic system (Allura Xper FD20; Philips Healthcare, Best, the Netherlands). This system was equipped with the XperCT option, enabling C-arm cone-beam CT acquisition and volumetric image reconstruction (Feldkamp back projection) (27). For each cone-beam CT scan, the area of interest was positioned in the system isocenter, and, over approximately 10 seconds, 312 projection images (30 frames per second) were acquired with the motorized C-arm, covering a 200° clockwise arc at a rotation speed of 20° per second. As the images were being acquired, the projections were transferred via fiber-optic connection to the reconstruction computer to produce volumetric data. The two-dimensional projection images were reconstructed by using Feldkamp back projection into three-dimensional volumetric images with isotropic resolution of 0.98 mm for a 250  $\times$  250  $\times$  194-mm field of view (matrix size, 256  $\times$  256  $\times$  198).

The dual-phase cone-beam CT prototype feature, which is vendor specific and not commercially available at present, allowed modification of the XperCT option to be able to obtain two sequential, back-to-back cone-beam CT scans so that images in both early or arterial and delayed or venous phases were captured by using only one contrast material injection (23–25). Specifically, the Philips Healthcare software prototype is written in C++ and allows modification of the standard image acquisition procedure in three ways: (a) Image acquisition can occur with both clockwise and counterclockwise C-arm

rotations, (b) image reconstruction of data from both scans occurs after the completion of both scans, and (c) both reconstructed data sets are displayed side by side and allow simultaneous cine viewing.

In our study, the two scans were triggered 3 and 28 seconds after a selective (segmental) single injection of undiluted contrast medium through a 3.0-F coaxial microcatheter placed in the main vessel expected to feed the targeted tumors on the basis of the location of tumors identified on baseline MR images. The final position of the microcatheter for delivery of the doxorubicin-eluting beads was based on the results of C-arm cone-beam CT. This was done to superselectively deliver the beads (via subsegmental arteries) to the tumors as often as possible. Each patient underwent only one dual-phase cone-beam CT examination before and after TACE after selective (segmental) injection of contrast medium. The same contrast material injection protocol was applied in all cases (amount, 20 mL; rate, 2 mL/sec; Oxilan, 300 mg of iodine per milliliter). The patients were instructed to be at end-expiration apnea during each of the cone-beam CT acquisitions, with free breathing between the early arterial and delayed venous phase scans. Oxygen was administered to patients during the procedure to minimize the discomfort of breath holding. One-millimeter isotropic images were immediately reconstructed in three dimensions from the dual-phase cone-beam CT scans and were reviewed routinely during the procedures.

### MR Imaging Technique

MR imaging was performed at baseline (within 6 weeks of initial TACE) and 1-month follow-up by using a 1.5-T unit (CV/I; GE Medical Systems, Milwaukee, Wis) and a phased-array torso coil. The imaging protocol included (a) axial T2-weighted fast spin-echo images (repetition time msec/echo time msec, 5000/100; matrix size, 256 × 256; section thickness, 8 mm; intersection gap, 2 mm; receiver bandwidth, 32 kHz), (b) axial single-shot breath-hold gradient-echo diffusion-weighted echo-planar

images (5000–6500/110; matrix size, 128 × 128; section thickness, 8 mm; intersection gap, 2 mm; b value, 500 sec/mm<sup>2</sup>; receiver bandwidth, 64 kHz), and (c) axial breath-hold unenhanced and contrast-enhanced (0.1 mmol/kg of intravenous gadodiamide [Omniscan, GE Healthcare, Princeton, NJ]) T1-weighted three-dimensional fat-suppressed spoiled gradient-echo images (5.1/1.2; field of view, 320–400 mm<sup>2</sup>; matrix size, 192 × 160; section thickness, 4–6 mm; receiver bandwidth, 64 kHz; flip angle, 15°) in the arterial and portal venous phases (20 and 60 seconds after intravenous contrast material administration, respectively).

### Imaging Data Evaluation

The MR images and dual-phase cone-beam CT scans were prospectively recorded and retrospectively evaluated offline at the end of inclusion. Images were interpreted in consensus by two experienced MR imaging and CT radiologists (R.L. and P.P.R., with 7 and 6 years of experience, respectively); these radiologists did not perform the TACE procedure. Image evaluation was conducted in the same reading session to ensure careful comparison of pre-TACE and sequential post-TACE MR imaging findings. The two radiologists assessed anatomic tumor response on T1-weighted contrast-enhanced MR images. In the same way, intraoperative dual-phase cone-beam CT images acquired before and after TACE were analyzed during a second reading session, 2 weeks later, where the readers were blinded to the MR imaging findings. Overall, interpretation of pre- and post-TACE MR images and dual-phase cone-beam CT scans was performed in a nonblinded manner. Some consideration was also given to the degree of reduction in contrast enhancement in terms of visual signal intensity, in addition to area measurements. For each session, however, radiologists were blinded to identities of the patients.

For each patient, we evaluated only the targeted tumor in cases of unifocal HCC and the two largest targeted tumors in cases of multifocal HCC to ensure independent sampling.

A radiologist (R.L.) used electronic calipers to record the size of the targeted tumors (one-dimensional measurement of the longest dimension, in keeping with RECIST guidelines) (12–14) on the portal venous phase MR images before and after TACE. A change in tumor size on MR images was calculated as a percentage change by using the following formula: [(longest dimension before TACE – longest dimension after TACE)/longest dimension before TACE] × 100%. The two radiologists visually assessed the percentage of tumor enhancement for the arterial phase MR images and early arterial phase dual-phase cone-beam CT scans and for the portal venous phase MR images and delayed venous phase dual-phase cone-beam CT scans in consensus. The percentage of enhancement was based on the percentage of the total area of enhancement seen on the axial image with the largest tumor size and was recorded subjectively in 5% increments, ranging from no enhancement to 100% enhancement. Consideration was also given to the degree of visual reduction in contrast enhancement in terms of signal intensity. Despite the fact that the volumetric measurements are likely to be more precise, this method is time-consuming. Consequently, we followed the current standards of qualitative measures applied to one representative axial section of the tumor, according to the EASL criteria.

Areas of tumor enhancement were considered an indication of viable tumor, as proposed by the EASL, and areas that were unenhanced were considered necrotic. Assessment of EASL score was limited to the two target lesions according to EASL guidelines. For each nodule, the percentage of tumor enhancement was assessed separately for dual-phase cone-beam CT and MR imaging according to EASL criteria. Relative change in tumor enhancement was divided into four categories: (a) complete disappearance of tumor enhancement (100% decrease) after treatment, denoting a complete response; (b) at least 50% decrease



in area of tumor enhancement, constituting a partial response; (c) at least 25% increase in area of tumor enhancement, indicating progressive disease; and (d) tumor enhancement changes that did not fit any of the previous three categories, including 0% decrease in area of tumor enhancement, designated as stable disease. An objective EASL response included complete response and partial response categories alone. For patients with two evaluated tumors, the lowest or worst EASL response score of the two tumors was used to classify EASL response in each patient.

### Radiation Dose Measurements

Radiation dose measurements were conducted in a porcine model to determine the amount of radiation imparted by an additional cone-beam CT scan in dual-phase cone-beam CT. One cannot simply double the dose from a single cone-beam CT examination to obtain dose measurements in dual-phase cone-beam CT because the C-arm movement geometry (clockwise and counterclockwise rotations) is different. This was done in one animal so that multiple dual-phase scans (10 overall) could be conducted with statistical power. Approval for this part of the study was obtained from the animal care and use committee. Radiation dose and exposure measurements were conducted in a 31.8-kg pig by using the same scanning conditions as those used in human subjects. Three measurements of dosimetry were acquired in the centerline of the CT path over the liver. For the dose measurements, two dosimeters (model DMC 2000 XB; MGP Instruments, Smyrna, Ga) were used, with one placed on top (entrance dose) of the pig and the other below (exit dose). The absorbed dose was calculated by subtracting the exit dose from the entrance dose. For the exposure measurements, the ionization chamber (model 451-P; Fluke Biomedical, Everett, Wash) was placed on the imaging table adjacent to the right side of the pig. Finally, the effective dose was calculated by multiplying

the absorbed dose by the liver tissue weighting factor (0.04).

### Statistical Analysis

All patient characteristic data at baseline were collected and reviewed before TACE, including demographics, HCC stage, results of serum tests, and radiographic findings. Data from AFP and radiographic evaluations 1 month after TACE were also collected. The primary statistical end point of this study was an area of tumor enhancement in the first and second phases at baseline and 1 month after therapy. All sample size calculations were based on a power of 80% and a significance level of  $P < .05$ . The initial sample size assumptions were based on the change in tumor enhancement 1 month after TACE. To determine if tumor enhancement as evaluated with dual-phase cone-beam CT changed immediately after TACE and whether it helped predict anatomic EASL tumor response at 1-month MR imaging follow-up, the post-TACE change in lesion enhancement for both imaging modalities was calculated as a difference between post- and pre-TACE scores according to the following formula: [(percentage tumor enhancement after TACE - percentage tumor enhancement before TACE)/percentage tumor enhancement before TACE]  $\times$  100. Correlations between post-TACE changes between modalities, which were performed separately for arterial and venous phases, were estimated by using the coefficient of determination ( $R$ ) obtained from regressing the change in lesion enhancement for MR imaging on the change in lesion enhancement for cone-beam CT. We fit models with tumor enhancement, tumor size, and AFP level as outcomes and an indicator for post-TACE findings to assess the average change after TACE for the two modalities and arterial and venous phases.

To account for the nesting of multiple lesions within patients, we used ordinary least squares estimation with Huber-White robust estimates of the variance (28). Complete, partial, and objective responses as defined with the EASL criteria were calculated by using MR imaging data. We used a marginal generalized

linear model with binomial distribution and logit-link to estimate the effect of lesion enhancement at dual-phase cone-beam CT after TACE on the probability of objective response at MR imaging. The model was estimated by using generalized estimating equations with empirical standard errors (29) and exchangeable working correlation structure to account for the within-patient correlation of multiple lesions. The effect of other patient- and tumor-related characteristics was also explored. The Lowess nonparametric smoother method was used to investigate the functional form of continuous covariates. An extension of the Hosmer-Lemeshow goodness-of-fit statistic for ordinary logistic regression to marginal regression models for repeated binary responses was used to assess the fit of the model (30). In addition, we inspected the area under the receiver operating characteristic curve of the true response status against the predicted probabilities of the response to assess the accuracy of the model.

All statistical analyses were performed by using software (Stata, release 11; Stata, College Station, Tex). Significance of statistical tests was assessed at the  $P < .05$  level.

## Results

### Patient Demographics

Twenty-seven patients with unresectable HCC (15 men, 12 women; mean age, 61.9 years  $\pm$  10.7; age range, 30–80 years) were included in our study. All patients successfully completed both baseline pre- and post-TACE dual-phase cone-beam CT and MR imaging. Each patient underwent one selective TACE session. All procedures were performed successfully, without immediate complications. The demographic data for this 27-patient cohort are summarized in Table 1. Nineteen of the 27 patients had multifocal HCC with preserved underlying liver function (Child-Pugh class A disease). Fifteen of the 27 patients (56%) had cirrhosis, and 12 (44%) had grade C Barcelona Clinic Liver Cancer (two patients had grade A, 10 had grade B, and three had grade D). Overall, 47

targeted lesions were evaluated (mean, 1.7 per patient; range, 1–2). Seven patients had one lesion and 20 had two lesions. The mean size of the targeted tumors at baseline was 70 mm ± 48 (range, 11–200 mm).

**Tumor Response at Follow-up MR Imaging: Assessment with EASL Criteria**

The contrast-enhanced T1-weighted MR images obtained at 1-month follow-up demonstrated an objective EASL response of complete response in 63% of patients and partial response in 70% of patients, as well as an objective response in 74% and 76% of tumors in the arterial and venous phases, respectively. The frequency of types of response according to modality and phase per patient and per tumor are detailed in Table 2.

**Tumor Enhancement Changes at Dual-Phase Cone-Beam CT and Prediction of Tumor Response**

Results of the paired *t* test to compare change in tumor enhancement after TACE according to modality and phase are presented in Table 3. The results are consistent with a significant decrease in tumor enhancement after TACE for both modalities and both phases (*P* < .0001). The decrease in tumor enhancement at cone-beam CT after TACE showed a linear correlation with MR imaging findings, and estimated correlation coefficients were excellent for both arterial (*R* = 0.89, *P* < .0001) (Fig 1a) and venous (*R* = 0.82, *P* < .0001) (Fig 1b) phases. With regard to tumor size, the results of the *t* test showed a significant decrease in the longest dimension of the tumors after TACE (*P* < .0001). There was no significant decrease in AFP level over time (*P* = .121).

Table 4 presents the results of marginal generalized linear models to estimate the odds or likelihood of objective response as a function of predictors: tumor enhancement at cone-beam CT after TACE, AFP level before TACE, and tumor size before TACE (by looking at the longest diameter). At bivariate analyses (looking separately at the effect of each of the predictors on the objective response),

**Table 1**

**Baseline Characteristics of Patients with HCC**

Parameter	Value
<b>Demographics</b>	
No. of patients	27
No. of tumors evaluated	47
Patient age (y)*	61.9 ± 10.7
<b>Sex</b>	
M	15
F	12
<b>Race</b>	
White	12
African-American	7
Hispanic	2
Other	6
<b>Etiology</b>	
Alcohol-related disease	2
Hepatitis C virus	12
Hepatitis B virus	2
Nonalcoholic steatohepatitis	2
Cryptogenic disease	9
<b>Eastern Cooperative Oncology Group performance status</b>	
0	15
1	10
2	2
3	0
4	0
<b>Cirrhosis</b>	
Present	15
Absent	12
<b>Disease type</b>	
Unifocal	6
Multifocal	12
Diffuse	9
<b>Portal venous thrombosis</b>	
Present	8
Absent	19
Tumor size (mm)*†	70 ± 48
<b>Child-Pugh class</b>	
A	19
B	6
C	2
<b>Barcelona Clinic Liver Cancer stage</b>	
A	2
B	10
C	12
D	3
<b>Okuda stage</b>	
I	11
II	15
III	1
<b>Cancer of the Liver Italian Program score</b>	
1	8
2	11

Table 1 (continues)

**Table 1 (continued)**

Baseline Characteristics of Patients with HCC	
Parameter	Value
3	5
4	2
5	1
Laboratory values*	
Basal AFP level (ng/mL)†	38 209 ± 176 640
Albumin level (g/dL)	3.6 ± 0.8
Total bilirubin level (mg/dL)	1.8 ± 3.4
Aspartate aminotransferase level (U/L)	129.6 ± 78.6
Alanine aminotransferase level (U/L)	103.8 ± 83.5
Alkaline phosphatase (U/L)	244.8 ± 260.7
International normalized ratio	1.2 ± 0.7

Note.—Except where indicated, data are numbers of patients.  
 \* Data are means ± standard deviations.  
 † One-dimensional measure of the longest dimension as measured with MR imaging.  
 ‡ The AFP level was less than 10 ng/mL in 10 patients, 10–20 ng/mL in eight, and more than 200 ng/mL in 10.

**Table 2**

Modality and Phase	Complete	Partial	Objective	Stable Disease	Progressive Disease
	Response	Response	Response*		
<b>Cone-beam CT</b>					
<b>Arterial phase</b>					
No. of patients	3 (11)	18 (67)	21 (78)	6 (22)	0 (0)
No. of tumors	7 (15)	30 (64)	37 (79)	10 (21)	0 (0)
<b>Venous phase</b>					
No. of patients	3 (11)	11 (41)	14 (52)	10 (37)	3 (11)
No. of tumors	10 (21)	17 (36)	27 (57)	17 (36)	3 (6)
<b>MR imaging</b>					
<b>Arterial phase</b>					
No. of patients	1 (4)	16 (59)	17 (63)	9 (33)	1 (4)
No. of tumors	3 (6)	32 (68)	35 (74)	11 (23)	1 (2)
<b>Venous phase</b>					
No. of patients	4 (15)	15 (56)	19 (70)	6 (22)	2 (7)
No. of tumors	13 (28)	23 (49)	36 (76)	8 (17)	3 (6)

Note.—Data were obtained in 27 patients and 47 tumors. Numbers in parentheses are percentages. Cone-beam CT was performed immediately after TACE. MR imaging was performed 1 month after TACE.  
 \* The objective response comprised the complete and partial responses.

tumor enhancement at cone-beam CT after TACE showed a negative association with the odds of an objective response in the arterial and venous phases. In the arterial phase, tumors with a 1% increase in enhancement on cone-beam CT scans after TACE had a 5% lower likelihood of achieving

objective response (95% confidence interval [CI]: 0.01, 0.09;  $P = .027$ ). In the venous phase, tumors with a 1% increase in enhancement at cone-beam CT after TACE had a 4% lower likelihood of achieving objective response (95% CI: 0, 0.07;  $P = .034$ ). Results of multivariate analyses indicated that

tumor enhancement at cone-beam CT after TACE had an independent, negative effect on the likelihood of objective response after accounting for pre-TACE AFP level and tumor size. We estimated that, for lesions of the same size and same pre-TACE AFP level but with a 1% increase in post-TACE cone-beam CT enhancement, the likelihood of objective response was lower by approximately 5% in the arterial phase (95% CI: 0.01, 0.09;  $P = .023$ ) and 4% in the venous phase (95% CI: 0.01, 0.07;  $P = .035$ ).

In addition, we saw a negative, significant, independent effect of pre-TACE AFP level on odds of objective response in the venous phase. For lesions of the same size and same post-TACE cone-beam CT enhancement level in the venous phase, the likelihood of objective response decreased by approximately 0.3% (95% CI: 0.1%, 0.4%;  $P = .003$ ) for tumors that had a 1000 ng/mL higher concentration of pre-TACE AFP. In these data, pre-TACE tumor size did not affect the likelihood of objective response after accounting for the pre-TACE AFP level and post-TACE cone-beam CT tumor enhancement ( $P = .810$  and  $.359$  for arterial and venous phases, respectively). Figures 2 and 3 show representative dual-phase cone-beam CT images illustrating HCC enhancement changes during TACE and corresponding EASL tumor response at MR imaging 1 month later.

**Goodness-of-Fit and Accuracy of Multivariate Logistic Regression Models**

In the arterial phase, the area under the receiver operating characteristic curve was 0.75 (95% CI: 0.57, 0.94). For the goodness-of-fit test, the predicted probabilities of response were divided into three groups. Within each group, the predicted probability of response was compared with the true response by using the  $\chi^2$  test statistic with two degrees of freedom. The resulting value of the test statistic ( $\chi^2 = 1.01$ ,  $P = .602$ ) provides no evidence that the model does not provide an adequate fit to the data.

In the venous phase, the area under the receiver operating characteristic

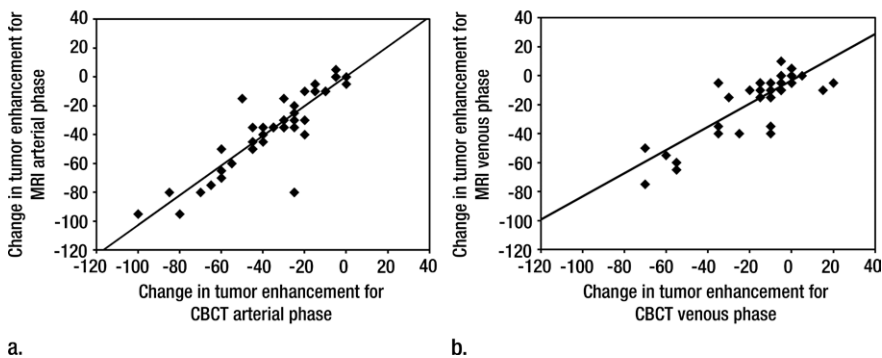
**Table 3****Changes in Tumor Size and Enhancement and Correlation with AFP Values after TACE**

Feature	Before TACE*	After TACE*	Percentage Change	P Value†
Tumor size (mm)‡	70 ± 48	66 ± 46	6	<.0001
Tumor enhancement at MR imaging (%)				
Arterial phase	56 ± 30	22 ± 22	61	<.0001
Venous phase	26 ± 25	11 ± 17	58	<.0001
Tumor enhancement at cone-beam CT (%)				
Arterial phase	54 ± 27	20 ± 19	63	<.0001
Venous phase	30 ± 27	15 ± 23	50	<.0001
AFP level (ng/mL)	38 209 ± 176 640	11 214 ± 43 947	71	.121

\* Data are means ± standard deviations.

†  $P < .05$  was considered indicative of a significant difference.

‡ One-dimensional measure of the longest dimension as measured with MR imaging.

**Figure 1**

**Figure 1:** Scatter plots show correlation of tumor enhancement changes in (a) early or arterial phase and (b) delayed or venous phase after TACE with doxorubicin-eluting beads, as measured with cone-beam CT (CBCT) and MR imaging. A decrease in tumor enhancement at cone-beam CT showed a linear correlation with findings at MR imaging. Estimated correlation coefficients were excellent for both arterial ( $R = 0.89$ ,  $P < .0001$ ) and venous ( $R = 0.82$ ,  $P < .0001$ ) phases.

curve was 0.73 (95% CI: 0.56, 0.90). For the goodness-of-fit test, the predicted probabilities of response were divided into two groups. The results of the  $\chi^2$  test ( $\chi^2$  with 1  $df = 0.29$ ;  $P = .593$ ) provide no evidence that the model does not provide an adequate fit to the data.

### Radiation Dosimetry

For the radiation dosimetry experiment conducted in the porcine model, the entrance dose was 1.42 mSv ± 0.01, the exit dose was 0.65 mSv ± 0.01, the absorbed dose was 0.77 mSv ± 0.0, and the exposure was 4.6  $\mu$ C/kg ± 0.5

per cone-beam CT scan (total for two dual-phase cone-beam CT scans: 5.68 mSv, 2.60 mSv, 3.08 mSv, and 18.4  $\mu$ C/kg, respectively). The effective dose for two dual-phase cone-beam CT scans was 0.12 mSv (liver tissue weighting factor, 0.04) (31).

### Discussion

Our study served to investigate whether dual-phase cone-beam CT can be used to predict tumor response obtained with MR imaging 1 month after TACE with doxorubicin-eluting beads in patients

with HCC. Our results showed that intraprocedural dual-phase cone-beam CT allowed monitoring and quantification of changes in tumor enhancement during TACE and assisted in accurate prediction of response to therapy.

Early determination of therapeutic response according to EASL criteria is helpful to guide patient treatment decisions after chemoembolization, especially with regard to the need for repeat treatment. Recently, vascular and cellular biomarkers, including contrast enhancement and apparent diffusion coefficients from diffusion-weighted MR imaging, have been shown to exhibit changes within tumors hours to days after therapy. Such changes typically precede those seen with anatomic imaging (according to World Health Organization or RECIST guidelines) (32–37). Nevertheless, to our knowledge, the optimum time for imaging and assessing tumor response after TACE remains unknown.

Some investigators have suggested that results of contrast-enhanced ultrasonography (US) performed at least 2 days after TACE could be predictive of tumor outcome (38), whereas others showed that findings at contrast-enhanced US performed 1 week after TACE were similar to those of dynamic CT performed 2 months after intervention (39). Several clinical studies have shown the ability of diffusion-weighted MR imaging to help map water distribution within HCC tumors and to help quantify tumor necrosis after transcatheter liver-directed therapy (36,40,41). Chung et al (42) also reported that intraprocedural apparent diffusion coefficient changes assessed in a hybrid angiography and MR imaging suite could help predict anatomic response at 1 month and thereby provide valuable feedback at the time of TACE. They found that patients whose intraprocedural apparent diffusion coefficients increase by more than 15% are more likely to have a favorable anatomic tumor response 1 month later.

None of the aforementioned studies, however, were able to address



Table 4

**Results of Marginal Generalized Linear Models Used to Predict the Probability of an Objective Response at 1-month MR Imaging as a Function of Covariates**

Variable	Simple Logistic Regression			Multiple Logistic Regression		
	Odds Ratio	95% CI	P Value	Odds Ratio	95% CI	P Value
<b>Arterial phase</b>						
Tumor enhancement at cone-beam CT after TACE*	0.950	0.910, 0.990	.027	0.950	0.910, 0.990	.023
AFP level before TACE†	1.010	0.900, 1.140	.839	1.004	0.997, 1.011	.264
Tumor size before TACE‡	0.999	0.984, 1.015	.946	0.998	0.986, 1.010	.810
<b>Venous phase</b>						
Tumor enhancement at cone-beam CT after TACE*	0.960	0.930, 1.000	.034	0.960	0.930, 0.990	.035
AFP level before TACE†	0.998	0.997, 0.999	.005	0.997	0.996, 0.999	.003
Tumor size before TACE‡	0.990	0.980, 1.000	.075	0.990	0.980, 1.010	.359

Note.— $P < .05$  was considered indicative of a significant difference. An objective MR imaging response was defined as complete and partial responses. Tumor response at MR imaging was assessed by using EASL guidelines.

\* For every 1% increment.

† Per 1000 ng/mL.

‡ One-dimensional measure of the longest dimension as measured with MR imaging.

the question of whether changes in tumor enhancement at chemoembolization could be used to predict EASL response (5,43). We were able to address this gap in knowledge with use of an integrated angiography and cone-beam CT suite. In comparison to other systems (angiography and MR units), our approach of using cone-beam CT has the added advantage of being readily available in many practices internationally. This suite enabled us to perform dual-phase cone-beam CT immediately before and after TACE, providing tumor imaging in both early arterial and delayed venous phases with use of only one contrast material injection. This was all accomplished without the need for multiple patient transfers, as reported when patients are moved between the DSA unit and the adjacent MR unit during the TACE procedure in centers with hybrid angiography and MR imaging suites (42). By using this setup, we were able to show that dual-phase cone-beam CT could be used intraoperatively to predict objective response 1 month after TACE with doxorubicin-eluting beads.

As mentioned earlier, contrast enhancement is a reflection of cellular viability (32–34), where areas of tumor enhancement are considered

viable and unenhanced regions reflect tissue necrosis. To assess tumor enhancement accurately, at the time of the TACE procedure we used C-arm CT, which enabled the acquisition of a three-dimensional data set generated from one rotational run with use of cone-beam CT principles (18–22). When compared with conventional DSA, cone-beam CT can provide additional useful information for patients undergoing TACE (18–22), including increased sensitivity in the detection of tumors and better visualization of nontarget organs. Furthermore, dual-phase cone-beam CT has a benefit over contrast-enhanced MR imaging in that cone-beam CT can be performed during the TACE procedure, with minimal additional effort than that required with DSA and fluoroscopy. This can provide live-image feedback not only on the TACE delivery catheter positioning and drug delivery amount but also on embolization success, as shown in our study.

The dual-phase approach in our study did not increase the predictive tumor response by more than a single acquisition during the arterial phase. However, our study demonstrates several potential clinical benefits of dual-phase cone-beam CT, namely the ability to image tumors in both

the early arterial phase (to show enhancement of tumor-feeding vessels) and the delayed venous phase (to show enhancement of tumor parenchyma). In this context, dual-phase cone-beam CT offers added reliability and capability in the detection and visualization of HCC by guaranteeing that at least one of the two phases (arterial or venous) will provide images of good quality (eg, in case of streak artifacts in the other phase). This feature can be especially useful in the setting of severe cirrhosis and/or in small tumors, which can be extremely difficult to visualize with the current technology available. Another advantage of using dual-phase cone-beam CT over obtaining two separate cone-beam CT scans (which could be done with current technology) is that dual-phase cone-beam CT uses only one intraarterial injection of contrast material. This improvement reduces the use of iodinated contrast material by 50% for the cone-beam CT component of the interventional procedure. Furthermore, the software prototype modifies the standard image acquisition procedure in three ways. The first modification eliminates the need to reset the C-arm to its starting rotation position, saving approximately 10 seconds. The second modification

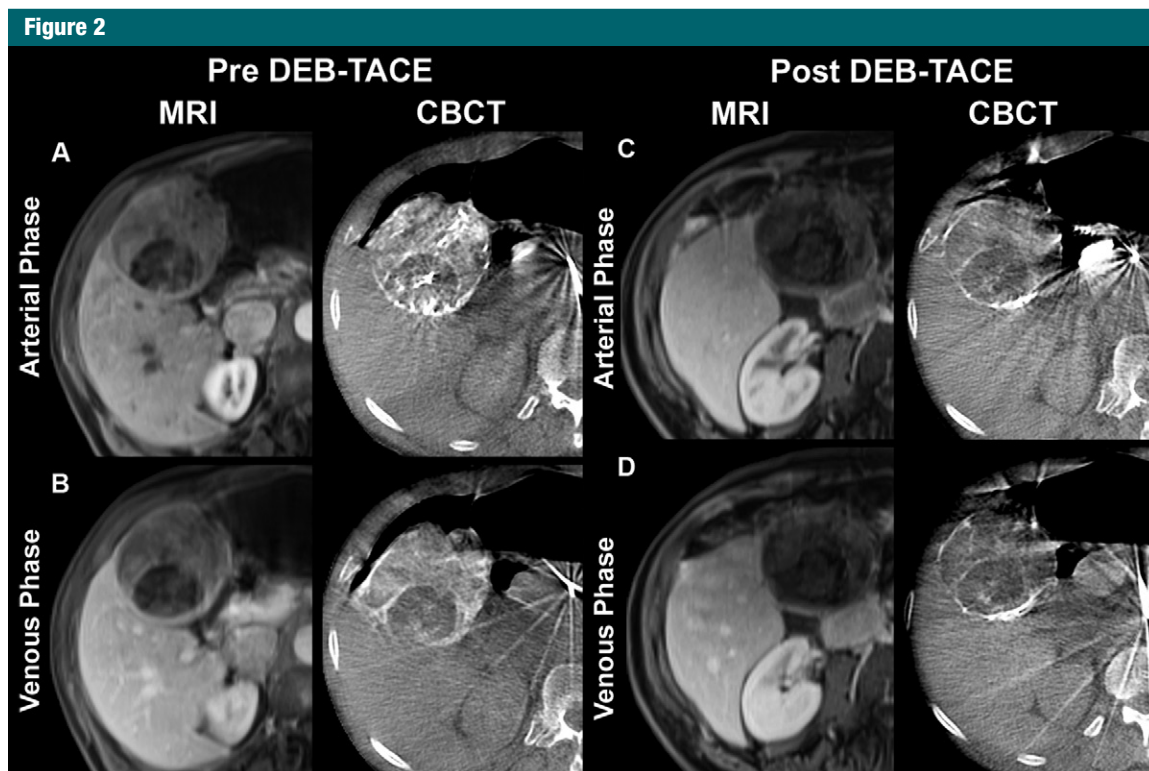


**Figure 2:** Representative T1-weighted axial contrast-enhanced arterial and portal venous phase MR images (*MRI*) and axial contrast-enhanced early or arterial phase and delayed or venous phase cone-beam CT scans (*CBCT*) in 73-year-old man with cryptogenic HCC in right lobe. MR images were acquired approximately 1 month before and 1 month after TACE with doxorubicin-eluting beads (*DEB*), whereas dual-phase cone-beam CT scans were acquired intraoperatively before and immediately after delivery of doxorubicin-eluting beads during TACE. *A*, Arterial phase images obtained before TACE. MR image shows a 75-mm mass in right lobe with 65% enhancement. Mass has similar enhancement (75%) on cone-beam CT scan. *B*, Venous phase images obtained before TACE. MR image shows mass with 60% enhancement. Similar enhancement (70%) is seen on cone-beam CT scan. *C*, Arterial phase images obtained after TACE. Mass shows almost no enhancement (5%) on MR image, and tumor has decreased to 69 mm. On cone-beam CT scan, intraprocedural mass enhancement decreased by 87%, which allowed prediction of an objective EASL response at 1 month. *D*, Venous phase images obtained after TACE. Mass shows no enhancement (0%) on MR image. Intraoperative enhancement decreased by 93% on cone-beam CT scan, enabling prediction of an objective EASL response at 1 month. As shown here, the patient has shifted in position between acquisition of the post-TACE MR images and the cone-beam CT images and pre-TACE MR images, which explains some differences in tumor size and morphology despite the fact that images were obtained at same level.

further saves time (approximately 60–90 seconds) by reordering the workflow. The approximate savings of 70–100 seconds creates the window for the second (delayed venous) scan to capture parenchymal enhancement by using the contrast material injected from the first phase. The third modification enables direct visual comparison between the two phases or between pre- and posttreatment images. This is an improvement over the standard software, where images from only one scan can be displayed at a time (23). Simultaneous visual comparison (early vs delayed) could

provide an idea of the vascular density of the tumor in relation to the feeding vessel.

Our study had several limitations. First, the sample was small, with possible selection bias because we included only 27 of 47 patients during the enrollment period. Our study only included patients who were undergoing their first TACE procedure. Findings in previously treated patients may have been different and may not correlate as well with those at post-treatment imaging. In addition, two patients with poor-quality dual-phase cone-beam CT scans were excluded

because of severe image artifacts. Second, we did not obtain data from histopathologic examination after treatment with TACE, meaning that there was no histopathologic correlation available with imaging regarding the degree of tumor necrosis present after treatment. Evidence of tumor necrosis was therefore measured only with MR imaging. Previous reports (32–34), however, have shown good correlation between the percentage of tumor necrosis obtained at histopathologic examination and the tumor enhancement assessed with MR imaging. Furthermore, interpretation

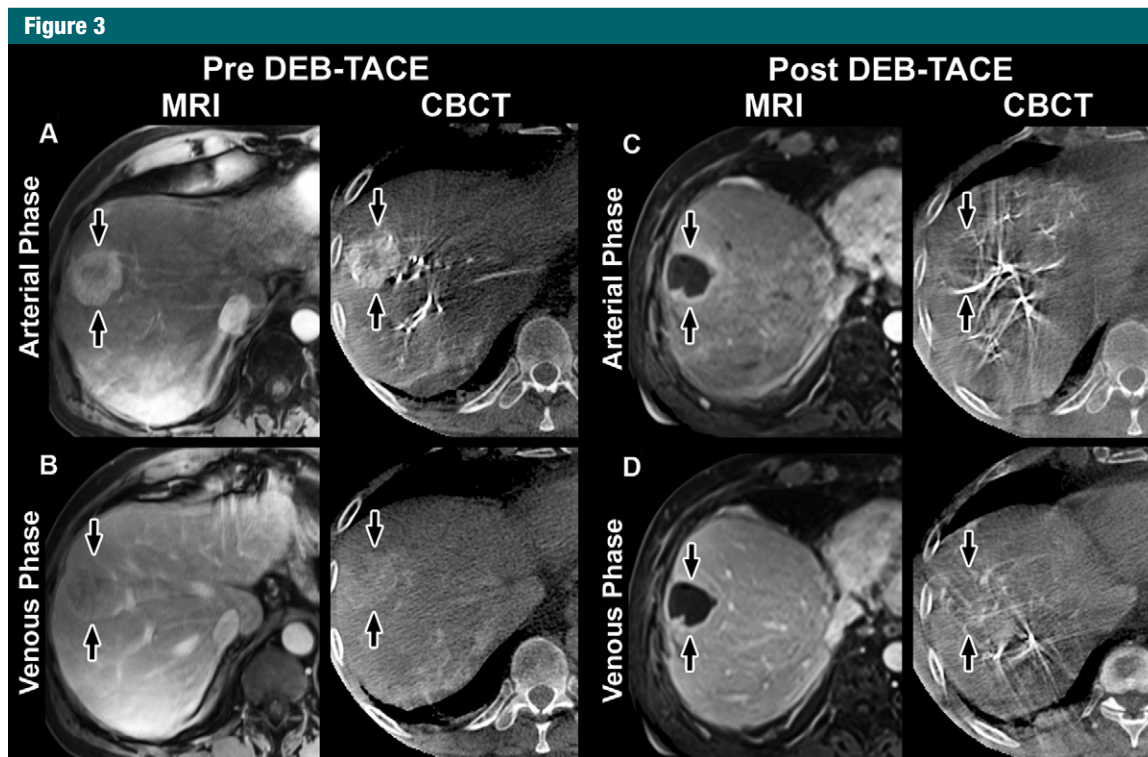


**Figure 3:** Representative contrast-enhanced arterial and venous phase MR images (*MRI*) and cone-beam CT scans (*CBCT*) in 58-year-old man with HCC in right lobe secondary to hepatitis C virus. MR images were acquired approximately 1 month before and 1 month after TACE with doxorubicin-eluting beads (*DEB*), whereas dual-phase cone-beam CT scans were acquired before and immediately after TACE. *A*, Arterial phase images obtained before TACE. MR image shows a 32-mm mass in right lobe with 75% enhancement (arrows). Cone-beam CT scan shows mass with similar enhancement (80%) (arrows). *B*, Venous phase images obtained before TACE. MR image shows mass with partial washout (50% enhancement) (arrows). Cone-beam CT scan shows mass with almost the same decrease in enhancement (65%) (arrows). *C*, Arterial phase images obtained after TACE. MR image shows mass with almost no enhancement (5%); tumor size remains unchanged (31 mm) (arrows). Cone-beam CT scan shows intraprocedural mass enhancement (arrows) decreased by 100%, which allowed prediction of objective EASL response at 1 month. *D*, Venous phase images obtained after TACE. MR image shows mass with almost no enhancement (5%) (arrows). Cone-beam CT scan shows intraprocedural mass enhancement (arrows) decreased by 92%, which allowed prediction of an objective EASL response at 1 month.

of MR and dual-phase cone-beam CT images obtained before and after TACE was conducted in a non-blinded manner. This might have introduced an element of bias. Third, it could be difficult to know whether an unenhancing portion of the tumor is due to good treatment or extrahepatic supply. However, because dual-phase cone-beam CT was performed immediately after the procedure, we did not consider recruitment of arterial supply from extrahepatic vessels by HCC tumors to be a factor. Conversely, monitoring the therapeutic effect with intraoperative cone-beam CT could have increased the

radiation dose. However, the effective radiation dose from cone-beam CT is substantially less than that of a typical abdominal scan with diagnostic multi-detector row CT (6.75 mSv for a pediatric abdominal interventional procedure), even when four cone-beam CT scans at a total of 3.08 mSv (two dual-phase acquisitions, one before and one after embolization) are obtained (44). Fourth, the cone-beam CT reconstruction might have accentuated substantial streak artifacts from catheters on cone-beam CT images when compared with conventional CT. This could have potentially limited accurate visual estimation of

tumor enhancement, especially in small lesions in the liver. New reconstruction and postprocessing methods are being developed to reduce artifacts. Furthermore, the use of visual estimation for tumor enhancement could have been a substantial limitation on its own. Another limitation is that this technology is a prototype in development by one vendor only and is not yet widely available. Finally, we do not yet have long-term follow-up evaluation of patient outcomes and cannot claim that patients with better tumor response have better clinical outcomes. The results of our study must be validated in future studies

with larger cohorts and longer follow-up times to determine whether tumor enhancement changes at intraoperative dual-phase cone-beam CT can reliably help predict patient prognosis or affect outcome.

In conclusion, our study showed that tumor enhancement changes at intraoperative dual-phase cone-beam CT could serve as a useful prognostic indicator of short-term HCC response to TACE with doxorubicin-eluting beads. Use of intraoperative dual-phase cone-beam CT at TACE could improve treatment planning, especially with regard to the need for repeat treatment. In particular, it could allow for complete treatment with further embolization during the procedure in case of persistent tumor enhancement at post-TACE dual-phase cone-beam CT. More important, a potential clinical implication of using intraoperative dual-phase cone-beam CT in these patients might be elimination of 1-month follow-up MR imaging.

**Disclosures of Conflicts of Interest:** **R.L.** Financial activities related to the present article: institution received a grant from Philips. Financial activities not related to the present article: none to disclose. Other relationships: none to disclose. **M.L.L.** Financial activities related to the present article: none to disclose. Financial activities not related to the present article: is an employee of Philips. Other relationships: none to disclose. **G.Y.** Financial activities related to the present article: none to disclose. Financial activities not related to the present article: received payment for manuscript preparation. Other relationships: none to disclose. **P.P.R.** No relevant conflicts of interest to disclose. **N.B.** No relevant conflicts of interest to disclose. **N.N.** Financial activities related to the present article: none to disclose. Financial activities not related to the present article: is an employee of Philips Healthcare. Other relationships: none to disclose. **A.R.** Financial activities related to the present article: none to disclose. Financial activities not related to the present article: is an employee of Philips Healthcare. Other relationships: none to disclose. **J.B.** Financial activities related to the present article: none to disclose. Financial activities not related to the present article: is an employee of Philips Healthcare. Other relationships: none to disclose. **E.L.** No relevant conflicts of interest to disclose. **J.F.G.** Financial activities related to the present article: none to disclose. Financial activities not related to the present article: is a paid consultant for Biocompatibles, Bayer HealthCare, Guerbet, Nordion, Merit, Abbott, and Jenne-rex. Other relationships: none to disclose.

## References

1. El-Serag HB, Rudolph KL. Hepatocellular carcinoma: epidemiology and molecular carcinogenesis. *Gastroenterology* 2007;132(7):2557–2576.
2. Bosch FX, Ribes J, Díaz M, Cléries R. Primary liver cancer: worldwide incidence and trends. *Gastroenterology* 2004;127(5 suppl 1):S5–S16.
3. Llovet JM, Real MI, Montaña X, et al. Arterial embolisation or chemoembolisation versus symptomatic treatment in patients with unresectable hepatocellular carcinoma: a randomised controlled trial. *Lancet* 2002;359(9319):1734–1739.
4. Lo CM, Ngan H, Tso WK, et al. Randomized controlled trial of transarterial lipiodol chemoembolization for unresectable hepatocellular carcinoma. *Hepatology* 2002;35(5):1164–1171.
5. Hong K, Khwaja A, Liapi E, Torbenson MS, Georgiades CS, Geschwind JF. New intra-arterial drug delivery system for the treatment of liver cancer: preclinical assessment in a rabbit model of liver cancer. *Clin Cancer Res* 2006;12(8):2563–2567.
6. Lewis AL, Gonzalez MV, Leppard SW, et al. Doxorubicin eluting beads. I. Effects of drug loading on bead characteristics and drug distribution. *J Mater Sci Mater Med* 2007;18(9):1691–1699.
7. Varela M, Real MI, Burrell M, et al. Chemoembolization of hepatocellular carcinoma with drug eluting beads: efficacy and doxorubicin pharmacokinetics. *J Hepatol* 2007;46(3):474–481.
8. Poon RT, Tso WK, Pang RW, et al. A phase I/II trial of chemoembolization for hepatocellular carcinoma using a novel intra-arterial drug-eluting bead. *Clin Gastroenterol Hepatol* 2007;5(9):1100–1108.
9. Malagari K, Alexopoulou E, Chatzimichail K, et al. Transcatheter chemoembolization in the treatment of HCC in patients not eligible for curative treatments: midterm results of doxorubicin-loaded DC bead. *Abdom Imaging* 2008;33(5):512–519.
10. Reyes DK, Vossen JA, Kamel IR, et al. Single-center phase II trial of transarterial chemoembolization with drug-eluting beads for patients with unresectable hepatocellular carcinoma: initial experience in the United States. *Cancer J* 2009;15(6):526–532.
11. Lammer J, Malagari K, Vogl T, et al. Prospective randomized study of doxorubicin-eluting-bead embolization in the treatment of hepatocellular carcinoma: results of the PRECISION V study. *Cardiovasc Intervent Radiol* 2010;33(1):41–52.
12. Therasse P, Arbuck SG, Eisenhauer EA, et al. New guidelines to evaluate the response to treatment in solid tumors. European Organization for Research and Treatment of Cancer, National Cancer Institute of the United States, National Cancer Institute of Canada. *J Natl Cancer Inst* 2000;92(3):205–216.
13. Tsuchida Y, Therasse P. Response Evaluation Criteria in Solid Tumors (RECIST): new guidelines. *Med Pediatr Oncol* 2001;37(1):1–3.
14. Lencioni R, Llovet JM. Modified RECIST (mRECIST) assessment for hepatocellular carcinoma. *Semin Liver Dis* 2010;30(1):52–60.
15. Bruix J, Sherman M, Llovet JM, et al. Clinical management of hepatocellular carcinoma: conclusions of the Barcelona-2000 EASL conference. European Association for the Study of the Liver. *J Hepatol* 2001;35(3):421–430.
16. Lim HK, Han JK. Hepatocellular carcinoma: evaluation of therapeutic response to interventional procedures. *Abdom Imaging* 2002;27(2):168–179.
17. Bruix J, Sherman M, Practice Guidelines Committee, American Association for the Study of Liver Diseases. Management of hepatocellular carcinoma. *Hepatology* 2005;42(5):1208–1236.
18. Kakeda S, Korogi Y, Ohnari N, et al. Usefulness of cone-beam volume CT with flat panel detectors in conjunction with catheter angiography for transcatheter arterial embolization. *J Vasc Interv Radiol* 2007;18(12):1508–1516.
19. Wallace MJ, Kuo MD, Glaiberman C, et al. Three-dimensional C-arm cone-beam CT: applications in the interventional suite. *J Vasc Interv Radiol* 2008;19(6):799–813.
20. Orth RC, Wallace MJ, Kuo MD, Technology Assessment Committee of the Society of Interventional Radiology. C-arm cone-beam CT: general principles and technical considerations for use in interventional radiology. *J Vasc Interv Radiol* 2008;19(6):814–820.
21. Miyayama S, Yamashiro M, Okuda M, et al. Usefulness of cone-beam computed tomography during ultraselective transcatheter arterial chemoembolization for small hepatocellular carcinomas that cannot be demonstrated on angiography. *Cardiovasc Intervent Radiol* 2009;32(2):255–264.
22. Miyayama S, Matsui O, Yamashiro M, et al. Detection of hepatocellular carcinoma by CT during arterial portography using a cone-beam CT technology: comparison with conventional CTAP. *Abdom Imaging* 2009;34(4):502–506.



23. Lin M, Loffroy R, Noordhoek N, et al. Evaluating tumors in transcatheter arterial chemoembolization (TACE) using dual-phase cone-beam CT. *Minim Invasive Ther Allied Technol* 2011;20(5):276–281.
24. Miyayama S, Yamashiro M, Okuda M, et al. Detection of corona enhancement of hypervascular hepatocellular carcinoma by C-arm dual-phase cone-beam CT during hepatic arteriography. *Cardiovasc Intervent Radiol* 2011;34(1):81–86.
25. Loffroy R, Lin M, Rao P, et al. Comparing the detectability of hepatocellular carcinoma by C-arm dual-phase cone-beam computed tomography during hepatic arteriography with conventional contrast-enhanced magnetic resonance imaging. *Cardiovasc Intervent Radiol* 2012;35(1):97–104.
26. Geschwind JF, Ramsey DE, Cleffken B, et al. Transcatheter arterial chemoembolization of liver tumors: effects of embolization protocol on injectable volume of chemotherapy and subsequent arterial patency. *Cardiovasc Intervent Radiol* 2003;26(2):111–117.
27. Feldkamp LA, Davis LC, Kress JW. Practical cone-beam algorithm. *J Opt Soc Am A Opt Image Sci Vis* 1984;1(6):612–619.
28. Williams RL. A note on robust variance estimation for cluster-correlated data. *Biometrics* 2000;56(2):645–646.
29. Diggle PJ, Liang KY, Zeger SL. *Analysis of longitudinal data*. New York, NY: Oxford University Press, 1994; 253–262.
30. Horton NJ, Bebchuk JD, Jones CL, et al. Goodness-of-fit for GEE: an example with mental health service utilization. *Stat Med* 1999;18(2):213–222.
31. The 2007 recommendations of the International Commission on Radiological Protection. *Ann ICRP* 2007;37(2-4):1–332.
32. Murakami T, Nakamura H, Hori S, et al. Detection of viable tumor cells in hepatocellular carcinoma following transcatheter arterial chemoembolization with iodized oil: pathologic correlation with dynamic turboFLASH MR imaging with Gd-DTPA. *Acta Radiol* 1993;34(4):399–403.
33. Castrucci M, Sironi S, De Cobelli F, Salvioni M, Del Maschio A. Plain and gadolinium-DTPA-enhanced MR imaging of hepatocellular carcinoma treated with transarterial chemoembolization. *Abdom Imaging* 1996;21(6):488–494.
34. Bartolozzi C, Lencioni R, Caramella D, Mazzeo S, Ciancia EM. Treatment of hepatocellular carcinoma with percutaneous ethanol injection: evaluation with contrast-enhanced MR imaging. *AJR Am J Roentgenol* 1994;162(4):827–831.
35. Ross BD, Moffat BA, Lawrence TS, et al. Evaluation of cancer therapy using diffusion magnetic resonance imaging. *Mol Cancer Ther* 2003;2(6):581–587.
36. Kamel IR, Liapi E, Reyes DK, Zahurak M, Bluemke DA, Geschwind JF. Unresectable hepatocellular carcinoma: serial early vascular and cellular changes after transarterial chemoembolization as detected with MR imaging. *Radiology* 2009;250(2):466–473.
37. Kalb B, Chamsuddin A, Nazzari L, Sharma P, Martin DR. Chemoembolization follow-up of hepatocellular carcinoma with MR imaging: usefulness of evaluating enhancement features on one-month post-therapy MR imaging for predicting residual disease. *J Vasc Interv Radiol* 2010;21(9):1396–1404.
38. Kono Y, Lucidarme O, Choi SH, et al. Contrast-enhanced ultrasound as a predictor of treatment efficacy within 2 weeks after transarterial chemoembolization of hepatocellular carcinoma. *J Vasc Interv Radiol* 2007;18(1 pt 1):57–65.
39. Xia Y, Kudo M, Minami Y, et al. Response evaluation of transcatheter arterial chemoembolization in hepatocellular carcinomas: the usefulness of sonazoid-enhanced harmonic sonography. *Oncology* 2008;75(suppl 1):99–105.
40. Kamel IR, Bluemke DA, Eng J, et al. The role of functional MR imaging in the assessment of tumor response after chemoembolization in patients with hepatocellular carcinoma. *J Vasc Interv Radiol* 2006;17(3):505–512.
41. Chen CY, Li CW, Kuo YT, et al. Early response of hepatocellular carcinoma to transcatheter arterial chemoembolization: choline levels and MR diffusion constants—initial experience. *Radiology* 2006;239(2):448–456.
42. Chung JC, Naik NK, Lewandowski RJ, et al. Diffusion-weighted magnetic resonance imaging to predict response of hepatocellular carcinoma to chemoembolization. *World J Gastroenterol* 2010;16(25):3161–3167.
43. Moschouris H, Malagari K, Papadaki MG, Kornezos I, Matsaidonis D. Contrast-enhanced ultrasonography of hepatocellular carcinoma after chemoembolisation using drug-eluting beads: a pilot study focused on sustained tumor necrosis. *Cardiovasc Intervent Radiol* 2010;33(5):1022–1027.
44. Racadio J, Yoshizumi T, Toncheva G, Stueve D, Anderson-Evans C, Frush D. Radiation dosimetry evaluation of C-arm cone beam CT for pediatric interventional radiology procedures: a comparison with MDCT (abstract). In: *Radiological Society of North America scientific assembly and annual meeting program*. Oak Brook, Ill: Radiological Society of North America, 2008; 638–639.